Hypersonic Modulation of Light in Three-Dimensional Photonic and Phononic Band-Gap Materials

A. V. Akimov,[1] Y. Tanaka,[2] A. B. Pevtsov,[1] S. F. Kaplan,[1] V. G. Golubev,[1] S. Tamura,[2] D. R. Yakovlev,[1,3] and M. Bayer[3]

[1]*A. F. Ioffe Physical-Technical Institute, St. Petersburg, 194021 Russia*

[2]*Department of Applied Physics, Hokkaido University, Sapporo 060-8628, Japan*

[3]*Experimentelle Physik II, Technische Universität Dortmund, D-44221 Dortmund, Germany*

(Received 20 November 2007; revised manuscript received 13 May 2008; published 18 July 2008)

The elastic coupling between the a-SiO_2 spheres composing opal films brings forth three-dimensional periodic structures which besides a photonic stop band are predicted to also exhibit complete phononic band gaps. The influence of elastic crystal vibrations on the photonic band structure has been studied by injection of coherent hypersonic wave packets generated in a metal transducer by subpicosecond laser pulses. These studies show that light with energies close to the photonic band gap can be efficiently modulated by hypersonic waves.

DOI: 10.1103/PhysRevLett.101.033902 PACS numbers: 42.70.Qs, 62.30.+d, 62.65.+k

The periodicity of the dielectric constants in artificially grown structures is generally accompanied by a periodicity of the acoustic impedance. With regard to their acoustic properties they may therefore behave as *phononic* crystals, in analogy to *photonic* crystals for light. If the structure acts as a photonic crystal operating in the visible, then it shows the features typical of phononic crystals for hypersonic ($\sim 10^{10}$ Hz) acoustic waves. The combination of optical and hypersonic properties in a single highly ordered periodic structure leads therefore to a new object comprising a photonic *and* phononic crystal. With such a joint system ultrafast manipulation and control of light beams by hypersonic waves in structures which have complete three-dimensional (3D) photonic and phononic band gaps may become feasible, promising a new generation of acousto-optical devices [1–3].

There are only a few papers in which the properties of submicrometer periodic structures have been described with respect to their photonic and phononic properties during the past decade [4–7]. Recently a step towards ultrafast manipulation of visible light using coherent hypersonic vibrations of the gold shell of *isolated* silica spheres in 3D photonic structures has been made [8]. These systems, however, do not provide a phononic band structure. To our knowledge coherent acousto-optical effects in which the elastic coupling between the elementary building blocks of the periodic structure is established have not been studied.

This Letter demonstrates modulation of visible light by "shaking" synthetic opals, well known as 3D photonic crystals, at a hypersonic frequency. The measured modulation spectrum contains frequencies characteristic for a strong mechanical coupling of the silica spheres composing the opal, which confirms that the studied structure behaves also as a phononic crystal. A theoretical analysis of the elastic vibrations in perfect opals predicts the vibrational modes which are involved in the light modulation when a coherent hypersonic wave packet is excited in a thin metal transducer.

The opal films with 1 cm^2 area were composed of close-packed silica spheres and grown by a vertical deposition method [9] on a silica substrate. The silica spheres formed a face-centered cubic (fcc) opaline matrix with the (111) plane parallel to the substrate surface. Two samples (1 and 2) were investigated. The silica sphere diameter in the colloidal suspension was $D = 359 \pm 10$ nm for both samples. From the scanning electron microscopy image in Fig. 1(a) it is seen that neighboring spheres are penetrating each other, which is a result of the sintering during the opal formation process. Thus there is a considerable elastic coupling, which may result in formation of a phononic band structure typical for phononic crystals. The elastic coupling parameter χ in the formed photonic-phononic crystal can be defined as $\chi = D/2a - 1$, where $2a$ is the distance between the centers of neighboring spheres [10].

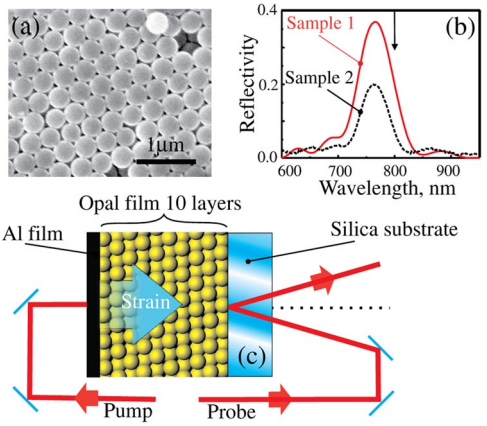

FIG. 1 (color online). (a) Scanning electron microscopy image of the opal film surface from which the sintering of spheres can be seen. (b) Optical reflectivity spectra of the opal film. The arrow indicates the wavelength of the probe light in the ultrafast experiments. (c) Setup of the pump-probe experiment.

The reflectivity spectra in Fig. 1(b) measured at room temperature demonstrate features typical for 3D photonic crystals [11]. The Bragg reflectivity peak with a maximum at $\lambda_m = 765$ nm arises from the stop band of the photonic crystal. The maximum reflectivity spectral position λ_m is given by $\lambda_m = 2d_0\sqrt{\varepsilon_0 - \sin^2\theta}$, where ε_0 is the mean permittivity of the opal structure, θ is the angle of light incidence, and $d_0 = 2\sqrt{6}a/3$ is the spacing between adjacent (111) lattice planes. The measured angular dependence of λ_m gives values of $d_0 = 290$ nm and $\varepsilon_0 = 1.74$. The obtained parameters were used to calculate the mean elastic coupling parameter [9], for which a value of $\chi = 0.015 \pm 0.005$ was obtained for both samples. The measured spectra [Fig. 1(b)] show oscillations due to Fabry-Perot interferences in the opal film. The oscillation periods correspond to film thicknesses of 10 and 12 silica sphere layers in samples 1 and 2, respectively.

The idea of the experiment [Fig. 1(c)] is to inject into the sample a picosecond coherent elastic wave packet from a hypersonic transducer and to make time-resolved measurements of the corresponding changes of the optical Bragg reflectivity spectrum. An aluminum film with a thickness of 100 nm was deposited on an opal sample surface. This metal film played the role of the hypersonic transducer for generation of a picosecond strain pulse to be injected into the opal film [12]. For excitation, 0.3 ps pulses from a Ti:sapphire laser with a regenerative amplifier ($\lambda =$ 800 nm, repetition rate 250 kHz, and maximum energy per pulse 1 μJ) were used. The pump beam was sent along a variable delay line and focused (200 μm spot diameter) on the metal transducer. The probe pulse was split from the same laser beam and was focused onto the silica substrate exactly opposite to the pump spot.

Figure 2(a) shows the measured reflectivity changes $\Delta R(t)/R_0$ for the two samples. R_0 is the reflectivity of the probe beam in the absence of pump excitation at a wavelength of 800 nm on a flank of the Bragg peak. After a sharp rise at $t = 0$, pronounced oscillations of $\Delta R(t)/R_0$ are observed. When the background is subtracted, in both cases the oscillatory part of the measured signal [Fig. 2(b)] cannot be described by a single period and depends on the sample.

Figure 2(c) shows the Fourier transforms of the oscillatory parts [Fig. 2(b)] of the measured signals $\Delta R(t)/R_0$. The peak (L) at $\nu_L = 11$ GHz is observed for both samples and has the highest amplitude. For sample 1 the peak L is accompanied by a low-frequency spectral wing while well-resolved peaks at 7 GHz (peak D) and 4 GHz (peak P) are seen for sample 2.

The origin of the oscillations in $\Delta R(t)/R_0$ is the elasto-optical effect. Coherent elastic vibrations modulate the period of the opal structure, which consequently results in modulation of the spectral position and width of the photonic stop band. When the probe light wavelength corresponds to one of the spectral wings of the Bragg reflection spectrum [as in our case in Fig. 1(b)] the efficiency of the hypersonic light modulation increases enormously [8]. This gives an essential advantage to the use of photonic-phononic crystals for light modulation over traditional acousto-optical materials.

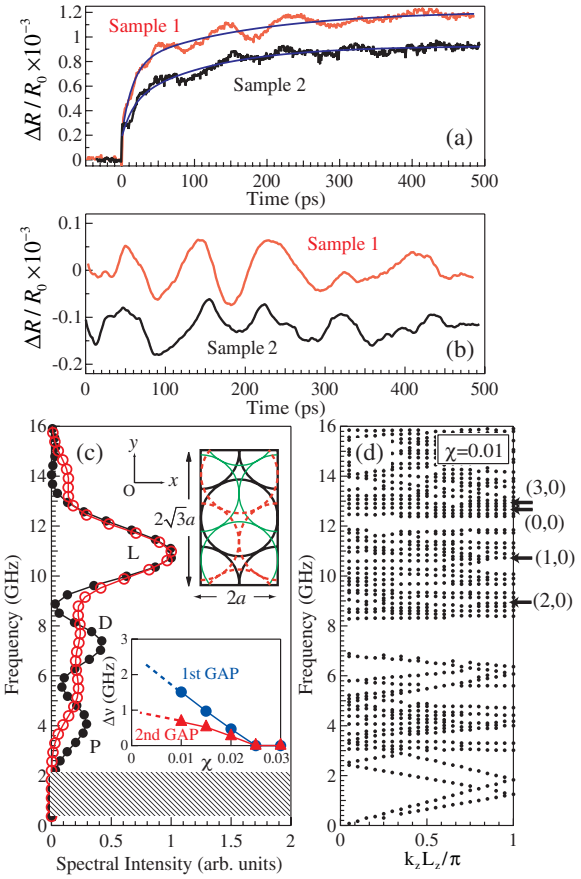

FIG. 2 (color online). (a) Measured $\Delta R(t)/R_0$ signals for the two samples. The smooth curves represent the slowly growing backgrounds. (b) Oscillatory parts of $\Delta R(t)/R_0$ (smoothed) after background subtraction. (c) Fourier transforms of the signals in (b). Open circles and dots correspond to samples 1 and 2, respectively. Hatched region is the frequency range where the results are not reliable. (d) Calculated band structure of the fcc infinite opal (with $\chi = 0.01$) along the $\Gamma - L$ direction. The arrows labeled by (l, n) are the eigenfrequencies of the low lying spheroidal modes in an isolated silica sphere. The upper inset in (c) shows the unit cell structure of an opal consisting of three layers of spheres (top, middle, and bottom layers are shown with thin green lines, dashed red lines, and bold black lines, respectively). The lower inset in (c) shows the width of the first (dots) and second (triangles) frequency gaps in (d) versus the parameter χ.

As a first approximation one may assume that the opal vibrational spectrum of a moderately coupled ($\chi \sim 0.01$) photonic-phononic crystal consists of modes with frequencies close to the eigenfrequencies of the isolated a-SiO_2 spheres, known as Lamb modes [13]. Theoretically, two families of Lamb modes, torsional and spheroidal ones, can be derived from the equations of motion for lattice displacements in an elastically isotropic sphere with a stress-free surface. The torsional modes leave the sphere

shape unperturbed and hence are not active in the modulation of the photonic-phononic crystal period and therefore the stop bands. The spheroidal modes, on the other hand, have mixed longitudinal and transverse character and their vibrations are associated with changes of the sphere volume. Consequently, we will limit our analysis to the spheroidal modes that can be classified in terms of the order l (angular momentum) of spherical Bessel functions $j_l(x)$ and an integer n indicating the number of nodes in radial direction. Accordingly we label the series of eigenfrequencies as $\nu_{l,n}$. Their values can be evaluated once the velocities of the longitudinal (L) and transverse (T) sound (for silica $s_L = 5.97 \times 10^5$ cm/s and $s_T = 3.77 \times 10^5$ cm/s, respectively [14]) and the radius of the sphere $r_0 = D/2$ are fixed. For spheres with $D = 359$ nm, the calculated frequencies of the spheroidal modes are shown by the horizontal arrows in Fig. 2(d). The experimentally observed L peak [Fig. 2(c)] has a frequency close to the purely radial mode ($l = 1, n = 0$) at $\nu_{1,0} = 10.8$ GHz. No distinct peak in the measured spectrum at $\nu_{2,0} = 9$ GHz which corresponds to the fundamental quadruple mode ($l = 2, n = 0$) is observed. This frequency would represent the lower limit, if the spheres were decoupled.

The exciting experimental fact is that the measured $\Delta R(t)/R_0$ spectrum [Fig. 2(c)] clearly shows vibrations with frequencies well below the lowest quadruple mode $\nu_{2,0}$. Elastic vibrations with frequencies below the Lamb modes can exist only if the vibrational modes spread over a distance exceeding the extension of an isolated sphere. Thus the experimental results clearly evidence that the spheres are considerably coupled with each other and the vibrational modes demonstrate phononic crystal behavior.

To obtain insight into the phononic crystal properties, we first study the effect of elastic coupling in perfect opals theoretically. The vibrational properties of phononic crystals have so far been studied with various methods, such as plane-wave-expansion [15], multiple-scattering [16–19], and finite-difference time-domain (FDTD) [20] methods. The first method has convergence problems, as a large number of plane waves are required when the elastic properties of the constituents are very different as in the present system (silica and vacuum). The second method has successfully been applied to the calculation of the vibrational band structure of opals in which silica spheres are separated from each other by air [19]. Unfortunately, this method cannot be applied to cases where the scatterers (i.e., the silica spheres) overlap.

The only viable and therefore applied method in our work is the FDTD approach even though the method is computationally cumbersome for 3D systems [21]. The calculated phonon dispersion curves along the [111] (z) direction for an infinite fcc opal are shown in Fig. 2(d). We have considered a rectangular parallelepiped unit cell with side lengths $L_x = 2a$, $L_y = 2\sqrt{3}a$, and $L_z = 2\sqrt{6}a$ in the x, y, and z directions, respectively, so that three layers of silica spheres are contained as shown in the upper inset of Fig. 2(c). For an elastic coupling parameter $\chi = 0.01$, which corresponds to the measured samples, there exists a complete phononic gap from 7.0 to 8.3 GHz. A second phononic gap is seen from 12.0 to 12.5 GHz. With increasing χ the volume of opal pores between the spheres becomes smaller and the structure evolves towards the acoustic properties of bulk silica. At around $\chi = 0.025$ [see the lower inset of Fig. 2(c)] the phononic gaps vanish. Very recently, a study of the phononic band structure in opals has been reported, in which band gaps in the phonon dispersions have been confirmed [22].

The temporal modulation of light in photonic-phononic crystals should follow the coherent hypersonic vibrations excited in the considered geometry [Fig. 1(c)]. To analyze the modulation we have calculated by FDTD simulations the spectral density of the elastic vibrations in an opal film consisting of ten layers of silica spheres on a silica substrate. We have also included the Al hypersonic transducer film at the top of the opal sample. Similar to the experimental situation we assume a short, coherent initial displacement over a large area of the Al film. Then, we average the relevant signals (after Fourier transformation into the frequency domain) over a large area of each silica layer in the opal film.

In Fig. 3 we plot the resulting spectral density for the difference of the displacement components u_z at the top and bottom edges of a sphere, i.e., $\Delta D_z \equiv u_z(z = +r_0) - u_z(z = -r_0)$. It is ΔD_z rather than u_z that contributes to changes of the photonic structure period and correspondingly to the spectral position of the photonic stop band and the modulation of light. There are several dips in which no phononic crystal modes are located: One dip extends from 4 to 9 GHz and another one with a width of 0.5 GHz is

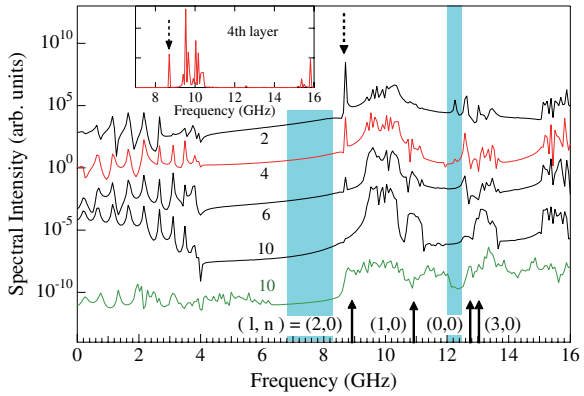

FIG. 3 (color online). Calculated spectral density of ΔD_z versus frequency of the ten layer opal film on a silica substrate. Upper four lines labeled by the layer number beginning from the metal film side are the results of the coherent excitation of an initial signal. Bottom line is obtained from a signal initially excited inside a sphere in the top layer. The spheroidal-mode frequencies in an isolated silica sphere are labeled by (l, n). The dashed arrow indicates the surface localized mode. Hatched regions correspond to the frequency gaps in Fig. 2(d). The inset shows the fourth layer spectrum on a linear scale.

centered at 12 GHz. Both of them are well correlated with the first and second vibrational gaps in the infinite system shown in Fig. 2(d). However, the first dip is much wider than the lowest frequency gap in the dispersion relation in Fig. 2(d).

For comparison, we also show in Fig. 3 a spectrum (the bottom line) resulting from an initial displacement u_z at a point inside a silica sphere, placed in the top layer. The lowest band now develops up to about 7 GHz. In this situation the lattice vibration is transmitted obliquely inside the opal film (like a spherical wave), producing a transverse vibration in addition to a longitudinal one. This result indicates that at the top of the lowest band (4–7 GHz) the vibrational modes are predominantly transverse in character.

An interesting feature in Fig. 3 is the existence of the spectral peak at about 8.7 GHz. This peak is prominent for layers near the surface where hypersonic waves are excited, but almost invisible at the tenth layer. Therefore, this should be a surface localized vibration, or more precisely a pseudosurface vibration which appears inside the band-gap and is often located close to the edge of a phononic crystal band [23,24]. A similar surface localized vibration is also seen inside the second band-gap.

The calculated spectra in Fig. 3 govern the spectrum of light modulation in a perfect photonic-phononic crystal. They are essentially different from the discrete spectrum of the isolated spheres (see vertical arrows in Fig. 3) and depend on the layer number in the opal film, as light with wavelength close to the photonic stop band can penetrate into the opal film over 10–20 layers [9]. This value is about the number of constituent layers in our synthesized photonic-phononic crystals. Thus all layers have to be taken into account in the considered geometry [Fig. 1(c)].

In summary, in 3D opal based photonic-phononic crystals light with a wavelength close to the photonic stop band can be strongly modulated by hypersonic vibrations with frequencies of about 10 GHz. The measured and calculated vibrational spectra consist of frequencies lower than the Lamb modes of isolated silica spheres. This underlines the importance of elastic coupling between the elementary blocks forming the 3D photonic-phononic crystal. Future experiments on opals with optimized homogeneity will give further insights into phonon dispersion and coherency [25]. The unification of photonic and phononic crystal structures may open the path towards new applications.

We acknowledge A. A. Kaplyanskii for fruitful discussions. The work was sponsored by the Russian Academy of Sciences, Russian Foundation for Basic Research (08-02-91960-a, 08-02-01171-a), PHOREMOST (FP6/2003/IST-2-511616), the Deutsche Forschungsgemeinschaft (Grant No. BA 1549/12-1), the CASIO Science Promotion Foundation, the Murata Science Foundation, the Grant-in-Aid for Scientific Research from the Ministry of Education, Science, Sports and Culture of Japan (Grant No. 17510106), and the Japan Society for the Promotion of Science.

[1] T. Gorishnyy, M. Maldovan, C. Ullal, and E. L. Thomas, Phys. World **18**, 24 (2005).
[2] M. Maldovan and E. L. Thomas, Appl. Phys. Lett. **88**, 251907 (2006).
[3] E. J. Reed, M. Soljacĉić, and J. D. Joannopoulos, Phys. Rev. Lett. **90**, 203904 (2003).
[4] P. Lacharmoise, A. Fainstein, B. Jusserand, and V. Thierry- Mieg, Appl. Phys. Lett. **84**, 3274 (2004).
[5] T. Gorishnyy, C. K. Ullal, M. Maldovan, G. Fytas, and E. L. Thomas, Phys. Rev. Lett. **94**, 115501 (2005).
[6] W. Cheng, J. J. Wang, U. Jonas, W. Steffen, G. Fytas, R. S. Penciu, and E. N. Economou, J. Chem. Phys. **123**, 121104 (2005).
[7] W. Cheng, J. J. Wang, U. Jonas, G. Fytas, and N. Stefanou, Nat. Mater. **5**, 830 (2006).
[8] D. A. Mazurenko, X. Shan, J. C. P. Stiefelhagen, C. M. Graf, A. van Blaaderen, and J. I. Dijkhuis, Phys. Rev. B **75**, 161102(R) (2007).
[9] J. F. Bertone, P. Jiang, K. S. Hwang, D. M. Mittleman, and V. L. Colvin, Phys. Rev. Lett. **83**, 300 (1999).
[10] G. M. Gajiev, V. G. Golubev, D. A. Kurdyukov, A. V. Medvedev, A. B. Pevtsov, A. V. Selkin, and V. V. Travnikov, Phys. Rev. B **72**, 205115 (2005).
[11] Y. A. Vlasov, X-Z. Bo, J. C. Sturm, and D. J. Norris, Nature (London) **414**, 289 (2001).
[12] G. Tas and H. J. Maris, Phys. Rev. B **49**, 15 046 (1994).
[13] H. Lamb, Proc. Math. Soc. London **13**, 189 (1882).
[14] Because of the porous nature of the silica spheres (see Ref. [10]) these values may be slightly ($<10\%$) smaller.
[15] M. S. Kushwaha, P. Halevi, L. Dobrzynski, and B. Djafari-Rouhani, Phys. Rev. Lett. **71**, 2022 (1993).
[16] M. Kafesaki and E. N. Economou, Phys. Rev. B **60**, 11 993 (1999).
[17] I. E. Psarobas, N. Stefanou, and A. Modinos, Phys. Rev. B **62**, 278 (2000).
[18] Z. Liu, C. T. Chan, P. Sheng, A. L. Goertzen, and J. H. Page, Phys. Rev. B **62**, 2446 (2000).
[19] I. E. Psarobas, A. Modinos, R. Sainidou, and N. Stefanou, Phys. Rev. B **65**, 064307 (2002).
[20] Y. Tanaka, Y. Tomoyasu, and S. Tamura, Phys. Rev. B **62**, 7387 (2000).
[21] For comparison, we calculated with the FDTD method the slope of the low-frequency limit of the dispersion curve for the fcc crystal consisting of polystylene spheres (not overlapping with a filling fraction of 30%) in water. The result is 1559 m/s, in good agreement with the 1566 m/s in effective medium approximation and the 1589 m/s in the multiple-scattering formalism as given in Ref. [19].
[22] T. Still *et al.*, Phys. Rev. Lett. **100**, 194301 (2008).
[23] Y. Tanaka and S. Tamura, Phys. Rev. B **58**, 7958 (1998).
[24] Y. Tanaka, T. Yano, and S. Tamura, Wave Motion **44**, 501 (2007).
[25] Another interesting way to see the coupling between the scatterers could be measurement and calculation of acoustic transmission spectra through the fcc layers. Then the resonant frequencies of an isolated sphere that are shifted and broadened by the couplings should manifest as dips or peaks in the transmission.